JOURNAL OF MATERIALS SCIENCE 27 (1992) 3192–3196

# Micro-analysis of welds using the field-ion microscope/atom probe

G. DUBBEN*, M. N. CHANDRASEKHARAIAH‡, B. H. KOLSTER
*Materials Science Section, Department of Mechanical Engineering, University of Twente, 7500 AE Enschede, The Netherlands*

Small addition of titanium and boron to welding consumables improves drastically the toughness of welded structures. To investigate the behaviour of titanium and boron on an atomic scale, an atom probe field-ion microscopic study was undertaken on two grades of welds; one with only titanium and one with titanium and boron. It was observed that boron forms pairs with carbon and small clusters with oxygen and carbon. The "bulk" composition in weight per cent was calculated for about 20 000 ions and showed considerable difference from the results obtained from other analytical techniques.

## 1. Introduction

High-strength offshore structured parts in the North Sea require a high level of notch toughness and crack opening displacement (C O D) properties of welded joints. During the last ten years new welding consumables have been developed. Addition of titanium and boron to consumables have been shown to improve the best impact properties of the weld metal considerably [1, 2] because they assist in increasing the percentage of fine-grained acicular ferrite in the microstructure of the weld metal. It is known that acicular ferrite improves the toughness drastically.

Titanium is known to suppress the effect of oxygen and nitrogen and protects boron against these elements. It is also known to help in the formation of small-scale inclusions and precipitates [3], which affect the acicular ferrite formation. Boron is known to suppress the $\gamma$-$\alpha$ transformation at austenite grain boundaries by segregating as free boron atoms [4] to these boundaries and reducing their interfacial energy. The optimum boron and titanium content depends on several factors, such as the weld chemistry, heat input, cooling rate, etc. Much controversy still exists concerning in what form boron is present at the prior austenite grain boundaries, whether it is as free boron or as boron-containing precipitates [5].

A clear understanding of the mechanism of titanium and especially boron in the weld metal depends on a quantitative evaluation of the distribution of these elements both in solid solution and across the interfaces. The field-ion microscope/atom probe, which combines a high sensitivity with excellent lateral and depth resolution, is the most appropriate technique to investigate this problem. Previous studies on austenitic steels [6] and low carbon steels [7] have established the viability of this technique in the study of grain-boundary segregation of boron. The present work reports the atom probe analysis of two grades of welds to make a comparative estimate of titanium and boron in solid solution.

## 2. Experimental procedure

Two multipass welds (one with only titanium, G45, one with titanium and boron, G46) prepared by gas-shielded $CO_2$ flux cored arc welding were selected for investigation. The material composition of the weld metal is given in Table I. The welds were prepared on 20 mm thick St-52 plates (Fig. 1), using a heat input of 1.9 kJ mm$^{-1}$ and they were air-cooled after welding.

Small sections, 25 mm × 5 mm × 5 mm, were cut out along the welds from the top layer and the secondary structure of the fifth pass. The cross-section of the welds was macro-etched to reveal the welded structure and the samples were carefully cut ensuring that the sections were from the fifth and eighth pass, respectively. Needles, 0.5 mm × 0.5 mm cross-section, were made from these sections by electro discharge machining. The needles were further thinned by electropolishing in 6% perchloric acid in acetic acid and the final field-ion specimens were prepared in 3% perchloric acid in butyloxy ethanol by zone polishing in a gold ring while observing in an optical microscope at a magnification of × 150.

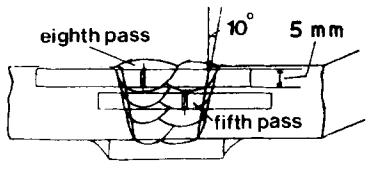


*Figure 1* Locations in the weld from where the specimens were taken.

* *Present address*: Ned. Philips Bedrijven B. V., Eindhoven, The Netherlands.
‡ *Present address*: Welding Research Institute, BHEL, Tiruchirapalli, India.


0022–2461 

TABLE I Chemical composition (wt %) of the welds

| | C | Mn | Si | P | S | Ti | B | O | N | Fe |
|---|---|---|---|---|---|---|---|---|---|---|
| G45 | 0.091 | 1.27 | 0.53 | 0.009 | 0.016 | 0.039 | – | 0.055 | 0.008 | bal |
| G46 | 0.087 | 1.37 | 0.61 | 0.009 | 0.017 | 0.051 | 0.0085 | 0.050 | 0.009 | bal |

Two different types of field-ion microscopes/atom probes were used. One consists of a straight time of flight mass spectrometer [8] and the other is a commercially available FIM 100 [9]. The specimens were imaged in neon gas (pressure $1.3 \times 10^{-3}$ Pa) at 90 K. The samples needed extremely careful handling. Several specimens failed intergranularly during field evaporation. As an example, Figs 2 and 3 show the electron micrographs of tips before and after their failure in the field-ion microscope/atom probe. The specimen failed during a sequence of controlled pulsed field evaporation and not due to sudden stress effects when the pulse voltage was switched on. Detailed micro-analysis was carried out by fixing the position of the probe hole at a desired area and taking a series of spectra. Typically, about 1000 ions were recorded in each spectrum with evaporation of about two atomic layers between each spectrum. Atom-probe analysis was also conducted to identify interesting features. In total about 20 000 ions (20 spectra) were recorded from the fifth and last pass each. The composition was evaluated in weight per cent for each spectrum and finally the average for the 20 spectra was taken as bulk composition.

## 3. Results

Figs 4 and 5 show typical field-ion images and the mass spectra from the two welds (top layers). A characteristic of all the field-ion images from the ferritic welds is the bright area around the {1 0 0} poles and a dark area around the {1 1 0} poles. These dark and bright areas persist during the entire sequence of field evaporation.

The mass spectra show clearly resolved peaks of all the isotopes of iron, namely $54Fe^{2+}$, $56Fe^{2+}$, $57Fe^{2+}$ and $58Fe^{2+}$ in their expected relative abundance. Carbon was observed as $12C^{2+}$ and $12C^{+}$, titanium as $48Ti^{2+}$ $48Ti^{+}$ and boron as $10B^{2+}$, $11B^{2+}$, $10B^{+}$ and $11B^{+}$. The nominal composition was worked out in weight per cent for each spectrum. It was observed from the experiments that the removal of about 1000 ions corresponds typically to about 20 atomic layers. The chemical composition in weight per cent for a sequence of 20 mass spectra is given in Table II for the eighth and fifth passes of the two grades G45 and G46.

From the field-ion images sometimes very bright spots appeared. This could be due to a kind of image promotion effect by residual gases. The size of these spots was about two to four atoms and they were

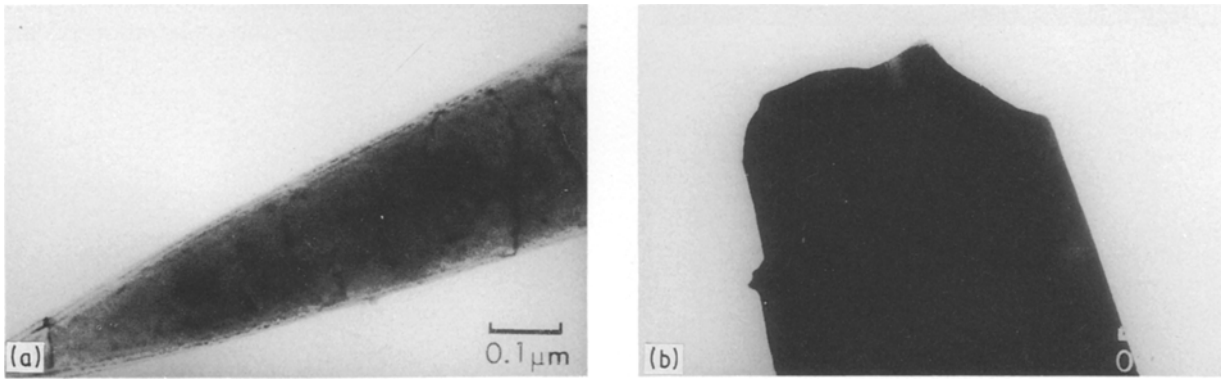


*Figure 2* Electron micrographs of the tip (a) before and (b) after their failure; notice the few dislocations in (a).

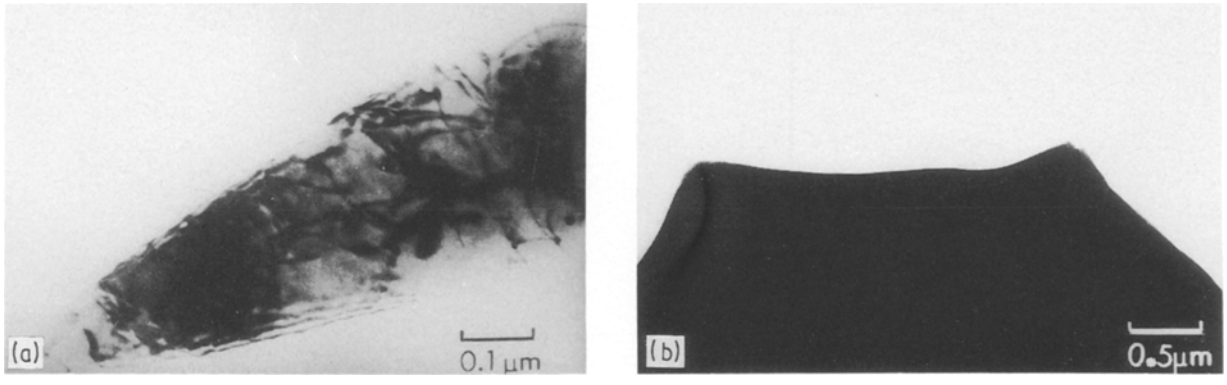


*Figure 3* Electron micrographs of the tip (a) before and (b) after their failure; notice the large amount of dislocations in (a).

observed for all the four samples. However, in several cases for both passes of G46 such bright spots could be analysed as clusters containing boron, oxygen and carbon (Fig. 6). During the analysis of the passes of G46, boron/carbon couples were also observed (Fig. 7).

## 4. Discussion

The weld specimen needed extremely careful handling, particularly in the initial stage of image formation. A number of specimens failed intragranularly during controlled pulsed evaporation. The fracture was located at the grain boundaries, far away from the imaging area (note the difference in magnification and tip diameter between Fig. 2a and b) where the regions of maximum stress exist (Fig. 2b). This was even true for a specimen with extremely high dislocation density near the tip (Fig. 3a). The fractured intergranular interface has pointed ends which could be similar to ledges observed in the dark-field electron micrographs of thin foils [10]. This evidence has been used to suggest a ledge mechanism of formation of acicular ferrite.

It is evident from the electron micrographs (Figs 2a and 3a) that the field-ion images are obtained from acicular ferrite grains. The high dislocation density was not seen in the field-ion images, partly because of lack of regularity in these images and partly because of migration of dislocations due to high stress fields. All the previous studies on boron-containing steels [6, 7] and metallic glasses [11] have reported the observation of boron peaks at $m/n = 5.0$, 5.5, 10 and 11, corresponding to charge states $10B^{2+}$, $11B^{2+}$, $10B^{+}$, and a higher abundance of single charge states at liquid nitrogen temperature [6, 7]. The results obtained from this investigation are in good agreement with these observations.

There are various opinions as to whether boron forms interstitial or substitutional solid solution in iron. Depending on the holding time and cooling rate from the austenite range, boron distribution occurs as segregant at the austenite boundaries and in intragranular regions. It has been established both theoretically and experimentally that diffusion of boron occurs as mobile boron–vacancy complexes [12]. These complexes can also be trapped by carbon, oxygen and nitrogen atoms and promote the formation of small clusters or couples. Clusters as well as couples were observed for the first time in this study which could be indirect experimental evidence for the proposed diffusion mechanism. Also the above mentioned factors account for the observation of large

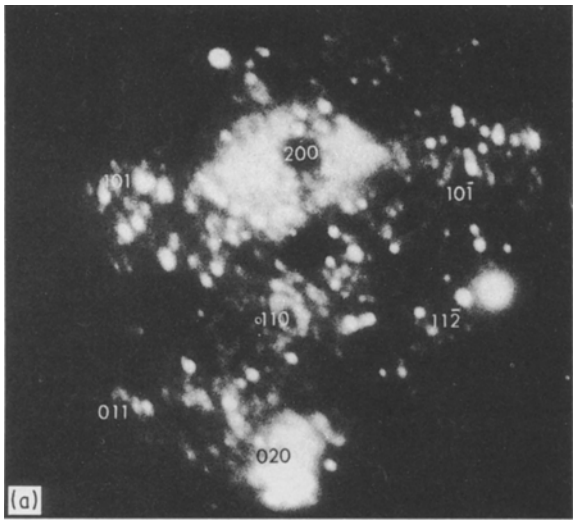


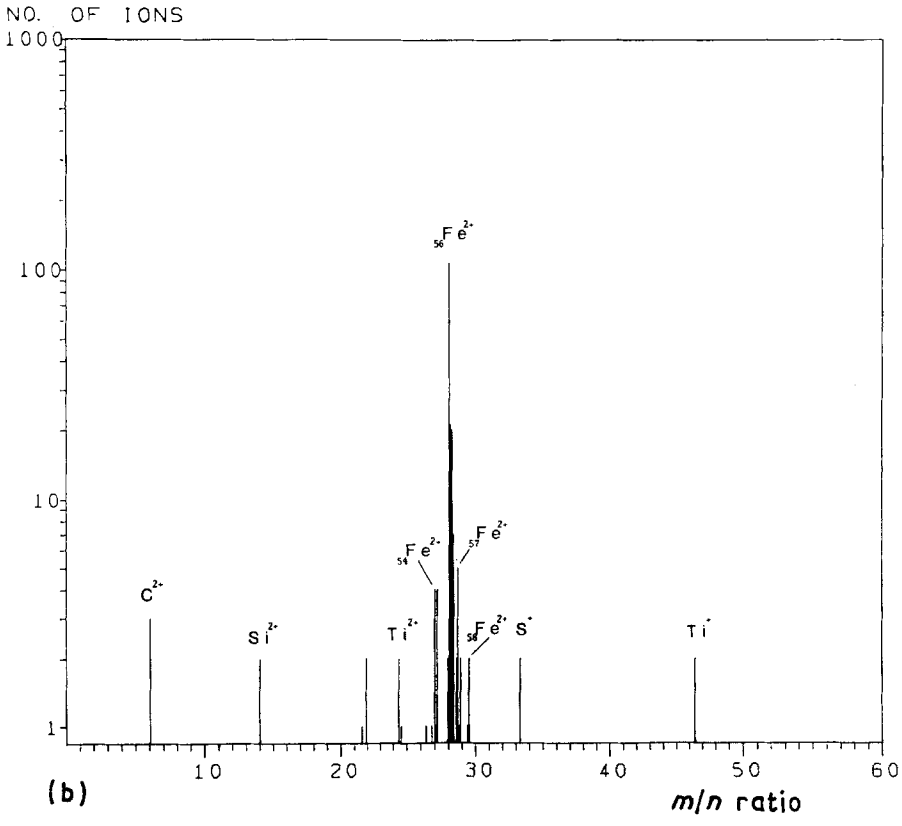


*Figure 4* (a) Field-ion image and (b) mass spectrum from the top layer of the titanium-containing weld metal (G45).

local concentration variations in boron, oxygen and carbon (cf. Table II).

Internal friction measurements of boron-containing HSLA steels did not show a Snoek peak for boron [13]. This provides strong evidence to suggest that boron does not form an interstitial solid solution in α-iron. Also, in that case, an increased carbon relaxation was observed in the presence of boron and this may be explained by the formation of substitutional boron–interstitial carbon pairs.

Our observation of boron–carbon pairs is direct experimental evidence for the above-mentioned concept. It should be noted that the boron concentration measured in the fifth pass is much lower than in the eighth pass. This may be explained by diffusion of boron to interfaces and grain boundaries during the heat cycle accompanying the subsequent weld passes. Large concentrations of boron are found in the bulk compared with the average chemical composition (compare Tables I and II). This observation has been explained [7] by assuming preferential segregation of boron to the surface during analysis of the specimen, the evidence being the decrease in boron concentration after field evaporation of ten atomic layers. The detailed depth analysis on the two passes of G46 did not show, however, a decrease in boron concentration. It remained constant within the statistical variation of the detection probability.

The boron solubility in α-iron has been reported to be around 20 to 30 p.p.m., based on hardenability results [5]. From autoradiographic studies, Brown *et al.* [12] report a solubility of 20 to 80 p.p.m. in α-iron and 55 to 260 p.p.m. in γ-iron. The atom-probe studies show a higher boron content, about 700 p.p.m. for the top layer and about 300 p.p.m. for the fifth pass, for

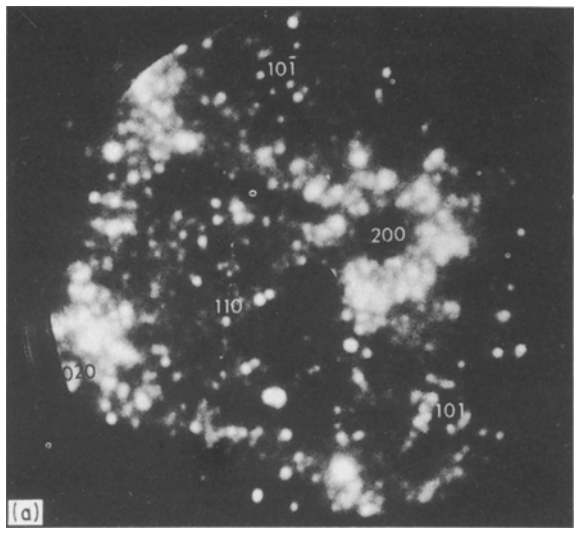


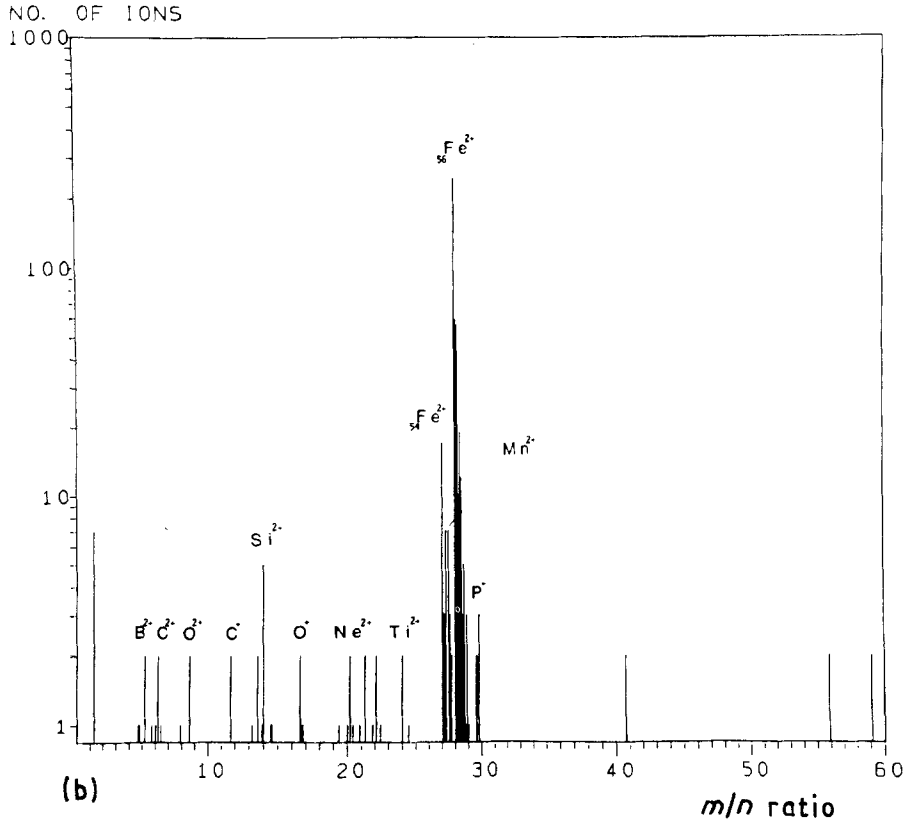


*Figure 5* (a) Field-ion image and (b) mass spectrum from the top layer of the titanium and boron-bearing weld metal (G46).

TABLE II Chemical composition (wt %) of the different passes determined by atom-probe microanalysis

| | Pass | C | Mn | Si | P | S | Ti | B | O | N | Fe |
|---|---|---|---|---|---|---|---|---|---|---|---|
| G45 | 8th | 0.068 | 1.20 | 0.46 | 0.064 | 0.076 | 0.17 | – | 0.076 | – | bal |
| | 5th | 0.083 | 1.47 | 0.39 | 0.083 | 0.083 | 0.19 | – | 0.083 | – | bal |
| G46 | 8th | 0.121 | 1.27 | 0.37 | 0.082 | 0.091 | 0.22 | 0.073 | 0.089 | – | bal |
| | 5th | 0.090 | 2.01 | 0.42 | 0.080 | 0.094 | 0.19 | 0.032 | 0.093 | – | bal |

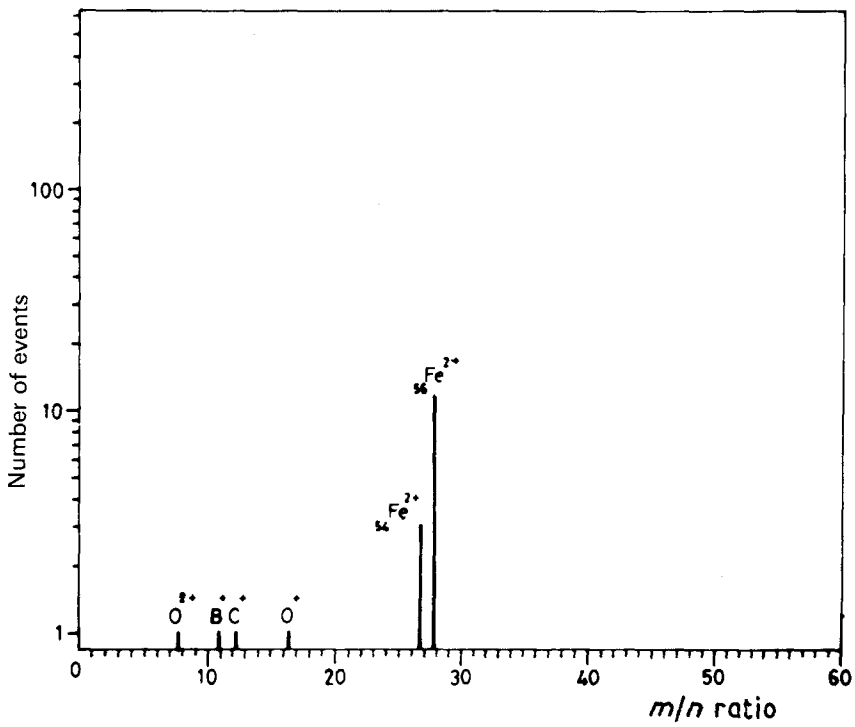


*Figure 6* Mass spectrum of a cluster in the top layer of weld metal G46.

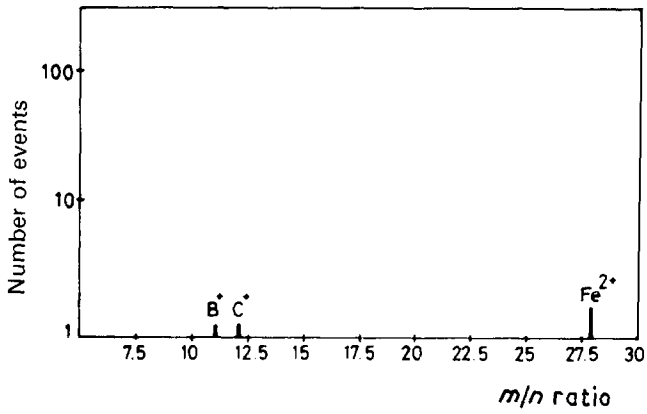


*Figure 7* Mass spectrum of a pair present in the top layer of G46.

which no straightforward explanation can be given. The only thing we can think of is statistics. Statistically, atomic scale analysis is bound to give a higher concentration because the detection of one boron ion in 100 or 1000 ions of iron gives a very high concentration in weight per cent. This, in fact, represents the limitation of micro-analysis of trace elements on an atomic scale, when a comparison has to be made with the bulk analysis of other methods.

## 5. Conclusions

1. Welded structures, including those containing trace amounts of titanium and boron are suitable for atom-probe micro-analysis.

2. The specimens can fail intergranularly due to the stress field and need careful handling.

3. Detailed micro-analysis in the interior of the grains indicate much higher concentrations for the trace elements boron, titanium and oxygen compared to the chemical analysis.

4. Boron forms clusters with oxygen and carbon and also couples with carbon.

## Acknowledgement

The authors thank Filarc Welding Industries (earlier Philips Welding Industries) for preparing the weld material and for their continuing interest in the work.

## References

1. H. HOMMA, N. MORI, S. SATIO and K. SHIMOYO, IIW Doc. IX-1072-78 (1978).
2. T. KOSHIO, M. OTAWA, T. TANIGAKI, T. TAKINO, T. HORII, E. TSUNETOMI and K. IMAI, IIW Doc. II-955-81.
3. C. THAULOW, paper 29. Proceedings of the Conference on Weld Pool Chemistry and Metallurgy, London (1980).
4. J. E. MORRAL and J. B. CAMERON, *Met. Trans.* **8A** (1977) 1817.
5. Ph. MAITREPIERRE, D. THIVELLIER, J. ROFÉS-VERMIS, D. RAUSSEAU and R. TRICOT, in "Hardenability concepts with applications to steel", edited by D. V. Doane and J. S. Kirkaldy, (Met. Soc. AIME 1978) p. 421.
6. L. KARLSON, H. -O. ANDRÉN and H. NORDÉN, *Scripta Metall.* **16** (1982) 297.
7. W. POLANSCHÜTS, *ibid.* **19** (1985) 153.
8. P. W. BACH and J. BEYER, in 26th International Field Emission Symposium Berlin (1979).
9. A. CEREZO, G. D. W. SMITH and A. P. WANGH, in 31st International Emission symposium Paris, July 1984.
10. R. A. RICKS, P. R. HOWELL and G. S. BARRITTE, *J. Mater. Sci.* **17** (1982) 732.
11. A. MENAND, C. MARTIN and J. M. SARRAU, *J. Physique* **95** (1984) C9.
12. T. M. WILLIAMS, A. M. STONEHAM and D. R. HARRIES, *Metal Sci.* **10** (1976) 14.
13. A. BROWN, J. D. GANISH and R. W. K. HONEYCOMBE, *ibid.* **8** (1974) 317.

*Received 3 January*
*and accepted 7 June 1989*